



Development of a CuNiCrAl Bond Coat for Thermal Barrier Coatings in Rocket Combustion Chambers

Torben Fiedler, Joachim Rösler, and Martin Bäker

(Submitted September 25, 2014; in revised form September 16, 2015)

The lifetime of rocket combustion chambers can be increased by applying thermal barrier coatings. The standard coating systems usually used in gas turbines or aero engines will fail at the bond coat/substrate interface due to the chemical difference as well as the different thermal expansion between the copper liner and the applied NiCrAlY bond coat. A new bond coat alloy for rocket engine applications was designed previously with a chemical composition and coefficient of thermal expansion more similar to the copper substrate. Since a comparable material has not been applied by thermal spraying before, coating tests have to be carried out. In this work, the new Ni-30%Cu-6%Al-5%Cr bond coat alloy is applied via high velocity oxygen fuel spraying. In a first step, the influence of different coating parameters on, e.g., porosity, amount of unmolten particles, and coating roughness is investigated and a suitable parameter set for further studies is chosen. In a second step, copper substrates are coated with the chosen parameters to test the feasibility of the process. The high-temperature behavior and adhesion is tested with laser cycling experiments. The new coatings showed good adhesion even at temperatures beyond the maximum test temperatures of the NiCrAlY bond coat in previous studies.

Keywords HVOF, NiCrAlY, NiCu, optical microscopy, porosity of coatings, thermal barrier coatings (TBCs)

1. Introduction

The combustion chamber of rocket engines has to withstand high thermal and thermomechanical loads. To allow for efficient cooling of the combustion chamber wall, it is usually made of a Cu alloy with high thermal conductivity. Liquid hydrogen in internal cooling channels cools down the chamber wall, but leads to a high thermal gradient. Additionally, the pressure difference between the cooling channels and the combustion chamber causes a high load on the thin sections. Due to this load and thermomechanical fatigue, the combustion chamber wall might fail by the so-called dog-house effect (Ref 1).

One idea to avoid this damage is to apply thermal barrier coatings (TBC) on the inside of the combustion chamber to reduce the temperature of the copper wall and hence reduce the thermal loads and thermal gradient in the wall.

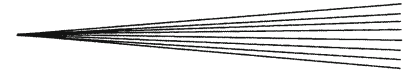
In the past, several different thermal barrier coatings were tested for rocket engine application (Ref 2, 3). Re-

cent work (Ref 4) focused on a ceramic top coat applied on a NiCrAlY bond coat, as used in gas turbines. The studies showed that this TBC system will fail in a rocket engine application. This failure is caused on the one hand by the higher chemical gradient due to the different substrate material compared to gas turbine application, where usually a Ni-based alloy is used with a chemical composition more similar to the bond coat material. This chemical difference lowers the chemical adhesion to the substrate and leads to a difference in thermal expansion between substrate and bond coat material. On the other hand, the high thermal gradient due to the higher cooling heat flux compared to the application in gas turbines causes higher internal stresses. It was therefore necessary to develop a new coating system.

The TBC system investigated in previous studies failed by delamination at the substrate/bond coat interface due to different thermomechanical properties of bond coat and substrate. Hence, the focus for the development of a new TBC system has to be on the development of the bond coat material. Recently, an alloy suitable as BC material was developed, based on the Cu-Ni-Cr-Al alloy system (Ref 5). This alloy has the composition Ni-30%Cu-6%Al-5%Cr. The coefficient of thermal expansion (CTE) is in the range between the CTE of the copper substrate and the CTE of possible top-coat materials like nickel or cobalt-rhenium alloys, while the high copper content reduces the chemical gradient at the substrate interface (Ref 5).

In this work, the feasibility of the coating application of the new NiCuCrAl alloy with high velocity oxygen fuel spraying (HVOF) is tested and suitable coating parameters are developed. The influence of these parameters on the coating process and the resulting coating structure was

Torben Fiedler, Joachim Rösler, and Martin Bäker, Institute for Materials, Technische Universität Braunschweig, Langer Kamp 8, 38106 Braunschweig, Germany. Contact e-mails: t.fiedler@tu-braunschweig.de, j.roesler@tu-braunschweig.de, and martin.baeker@tu-braunschweig.de.



investigated previously for MCrAlY and copper coatings (Ref 6-8). In (Ref 6), MCrAlY coatings are investigated. It is observed that the coating porosity is lowered at shorter spray distances due to the higher particle velocity. The particle velocity is measured in (Ref 7) for different spray distances. It increases with shorter spray distances, but decreases then below a critical distance. The porosity can furthermore be decreased by increasing the particle temperature and therefore the degree of melting of the powder particles. This can be done by increasing the spray distance, as observed in (Ref 7), or by increasing the flame temperature by varying the oxygen/fuel ratio (Ref 6). The oxygen/fuel ratio does not influence the particle velocity, as measured in (Ref 8).

In the present work, a parameter study on NiCuCrAl coatings is carried out based on the findings in the literature. The parameters mostly discussed in the literature (Ref 6-9), spray distance, oxygen/fuel rate, and combustion chamber pressure, are varied to investigate the influence on the coating structure of the new coating material.

2. Experimental Details

2.1 Coating Process

The coatings in this study were applied by high velocity oxygen fuel (HVOF) flame spraying. In this process, the coating material is injected as powder in a combustion flame, in this case a kerosene-oxygen flame. The powder particles reach velocities up to 1020 ms^{-1} (Ref 9). Since the accelerated particles stay in the flame for a very short time only, due to the high velocity, oxidation is less than in other atmospheric coating processes. Furthermore, the high particle velocity leads to a dense coating structure. Hence, the HVOF coatings reach a porosity and an oxide content lower than 2% (Ref 9, 10).

To determine the influence of the spray parameters on coating properties like porosity, roughness, or amount of unmolten particles in the coating, $60 \times 60 \times 3 \text{ mm}$ mild steel (S235) plates were used as substrates, since only the coating structure and not the influence of the substrate is investigated in the parameter study. The surface preparation of the substrate is of crucial importance for a good adhesion of the coating. On the one hand, an adequate surface roughness increases the mechanical adhesion, and on the other hand, a clean surface enhances the chemical adhesion of the applied coatings. In this study, the samples were grit blasted with aluminum oxide ($60\text{--}120 \text{ }\mu\text{m}$). In the blasting process, the substrate surface is roughened, and corrosion or thick oxide layers are abraded. To remove remaining abrasive particles or dust, the substrate samples were ultrasonically cleaned in ethanol.

The parameters established in this way were then used to produce coatings on copper. A CuCr1Zr alloy as used in previous studies (Ref 4) was used as substrate material. Coin-shaped samples with a height of 2 mm and a diameter of 20 mm were prepared in the same way as the steel substrates and then coated on one of the flat sides.

A WokaStar-610 HVOF gun from Sulzer Metco with a 4-inch barrel was used for coating application. The gun was moved with a 6-axis manipulator in a translative path over the substrate. A preheating of the samples was not carried out, since the copper substrate to be used in further studies would oxidize at elevated temperatures.

2.2 Characterisation of the Coatings

The coated samples were cut in cross section perpendicular to the coated surface. The cross section was ground and polished in several steps (9, 6, 3, and $1 \text{ }\mu\text{m}$) to investigate it with optical microscopy. At polishing steps finer than $3 \text{ }\mu\text{m}$, the observed porosity appears increased in the optical micrographs due to break-outs of small, poor adhering particles. Hence, the porosity of the samples had to be measured after the $3 \text{ }\mu\text{m}$ step. The polished surface remains still scratchy at this preparation step, but with the used image analysis tool ImageJ (Ref 11), it is possible to consider only the pores and not the scratches in the porosity measurement.

The coating thickness is measured at 100 points over a length of 15 mm with optical microscopy using an Olympus BX51 M microscope and the microscope software Stream Motion. The roughness R_q was calculated from these measurements. Unmolten particles were counted in a micrograph of a cross section of the coating over a length of 10 mm.

2.3 Laser Cycling Experiments

To test the adhesion of the coatings on copper substrates under a high thermal gradient and with high heating rates, a laser test bed was used. This method has been described elsewhere in detail (Ref 4). It consists of a high power diode laser with a broad focal point to heat up the surface of coated specimens homogeneously. The surface temperature of the coating is controlled by a pyrometer. In one cycle, it is ramped in 0.5 s to a specified value (here: 1000 and $1100 \text{ }^\circ\text{C}$), held constant for a fixed time (here: 2 and 10 s), until the laser is shut off for cooling. The fast heating results in a temperature difference between top and bottom of the specimen of up to 500 K.

3. Results and Discussion

The main requirements on the bond coat are a low porosity and a low oxide content as well as an adequate roughness. Pores and internal oxides lower the internal strength and, hence, the cohesion of the coating. A high surface roughness of the bond coat increases the adhesion of the top coat, but if the bond coat surface is too rough, it increases the roughness of the top-coat surface. Additionally, the interface may become too porous if a second layer is applied to a too rough surface.

The coating porosity, oxide content, and surface roughness vary with the coating parameters. Since the CuNiCrAl alloy is a new coating material, there have been

Table 1 Coating parameters investigated in this study

Fuel flow, L/h	Oxygen flow, slpm	Equivalence ratio ϕ (-)	Combustion chamber pressure p, MPa	Spray distance, mm
16.2	800	0.6	0.59	400
16.2	740	0.7	0.57	400
18.0	800	0.7	0.61	400
16.2	650	0.8	0.45	150..600 (in 50 mm steps)
18.0	740	0.8	0.59	400
20.0	800	0.8	0.64	400
18.0	650	0.9	0.54	400
20.0	740	0.9	0.61	400
22.0	650	1.0	0.57	400

no coating tests before and suitable coating parameters are not known yet. It is therefore necessary to do parameter studies with the coating process. The most important parameters are discussed in the following, and an overview of all parameters used for the study is listed in Table 1.

3.1 Size and Shape of the NiCuCrAl Powder

The shape and the size of the powder have a great influence on the coating process. A large particle size leads to a rough, porous coating, while powder particles smaller than 10 μm cause process instabilities like adhering powder in the barrel of the HVOF gun. Furthermore, the particle size influences the in-flight oxidation: The oxygen content of the coating increases strongly with decreasing particle size (Ref 12).

For the present process, a minimum powder size of 20 μm was found to be sufficient to enable a stable coating process with no powder adhesion in the coating gun and a stable powder conveyance. Since the powder atomisation is a statistical process, the range of the particle size accepted for coating must be large enough, to avoid that too much powder has to be sieved out and thrown away. So, the upper size limit was defined 50 μm , where a crop of approximately 50% of good powder was estimated.

The optimum shape of the powder particles is spherical with a smooth surface. A rough particle surface leads to a higher oxidation due to the larger surface area. Furthermore, the conveyance process of the powder is much easier with spherical particles.

The Ni-30%Cu-6%Al-5%Cr alloy developed in previous studies (Ref 5) was atomised in an argon flow at the company NANOVAL and sieved to the required size of 20 to 50 μm . The mean particle size is 28.8 μm , measured with laser diffraction at NANOVAL.

Figure 1(a) shows a scanning electron microscopy (SEM) image of the powder particles. They have a smooth, spherical shape, as required for the coating process. In Fig. 1(b), the cross section of a NiCuCrAl particle is shown. Here, a dendritic microstructure is visible. No internal cracks or pores were observed.

3.2 Variation of Spray Distance

The spray distance controls the flight time of the particles in the flame and, therefore, the heating and acceleration. Furthermore, short spray distances heat up the

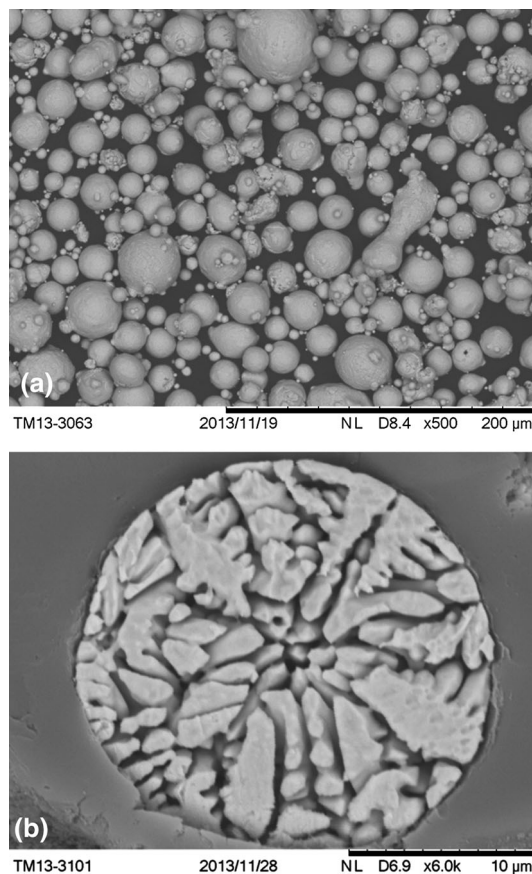


Fig. 1 SEM images of the powder particles of the alloy Ni-30%Cu-6%Al-5%Cr. (a) Particle shape and size. (b) Cross section of a single particle

substrate and the deposited coating. To find the optimum spray distance, different values in the range of 150 to 600 mm were investigated. The fuel flow (16.2 L/h) and oxygen flow (650 slpm) were kept constant. The resulting equivalence ratio for these flow rates is 0.8, the measured combustion chamber pressure is 0.45 MPa.

Figure 2 shows the measured values for porosity and roughness of the coatings deposited with different spray distances. The micrographs of some of the coatings are shown exemplarily in Figure 3. The porosity has the lowest values at spray distances between 250 and 500 mm. At longer spray distances, the porosity increases and reaches a level of 5% at a spray distance of 600 mm. The same

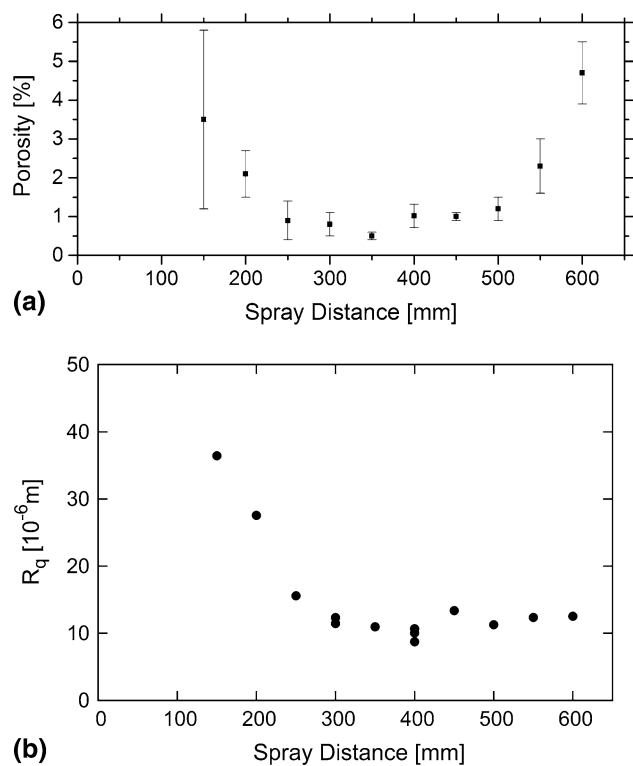


Fig. 2 Coating roughness and porosity at different spray distances. Fuel flow: 16.2 L/h, oxygen flow: 650 slpm. (a) Porosity of the coatings at different spray distances. (b) Roughness of the coatings at different spray distances

behavior was observed in (Ref 6) and explained by a decreasing particle velocity with increasing spray distance, as measured in (Ref 7). This reduces the impact of the particles on the coating surface and, thus, reduces its density. The observed increase of porosity below a spray distance of 250 mm might be caused on the one hand by the short particle-acceleration time due to the short flight time in the flame, as measured in (Ref 7). On the other hand, the short flight time leads to less heat transition in the particles, resulting in a lower particle temperature, as also observed in (Ref 7). Furthermore, at short spray distances, some particles were observed to spread away nearly parallel to the specimen surface, indicative of a relatively high amount of unmolten particles due to the low particle temperature.

Big oxide clusters were only observed at spray distances below 200 mm, as in Fig. 3(a), while the oxides at spray distances at 250 mm and above were only observed as thin stringers around the splats in the coating (Fig. 3b). These oxide stringers may be caused by the in-flight oxidation of the particles, as discussed in detail by Li et al. in (Ref 12). Their content increases normally with increasing flight time, but this interdependence could not be assessed in this work, since the oxide content was at a very low level for all larger spray distances. The big oxide clusters at short distances may not be caused by the in-flight oxidation due to the relatively short flight time of the parti-

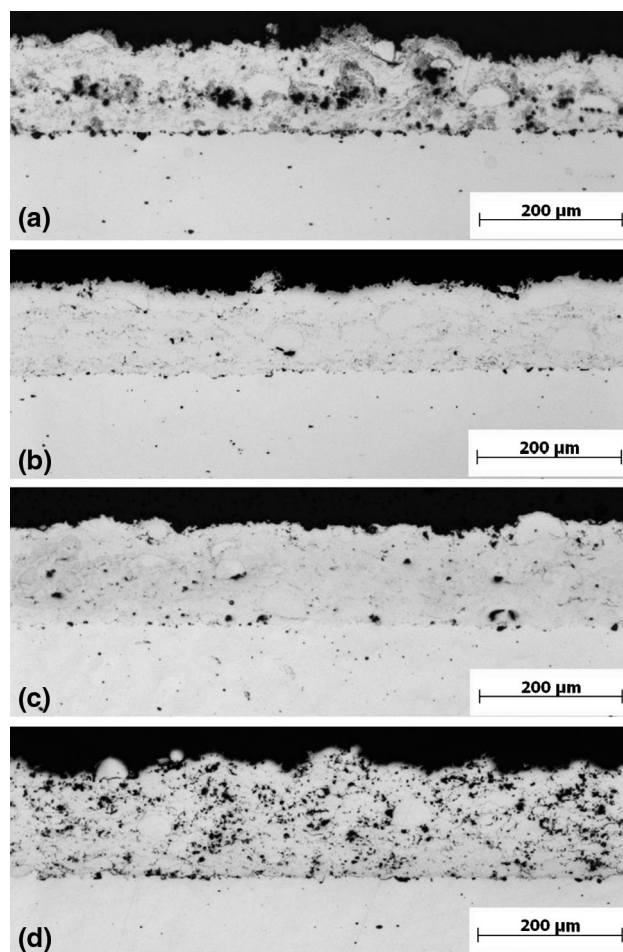


Fig. 3 Cross section of the CuNiCrAl coatings at different spray distances. Fuel flow: 16.2 L/h, oxygen flow: 650 slpm. (a) 150 mm spray distance. (b) 300 mm spray distance. (c) 400 mm spray distance. (d) 600 mm spray distance

cles, but rather by an oxidation of the already deposited coating due to the high temperatures of the sample during coating application, as seen in Fig. 3(a): oxidation can be observed mainly at the surface of the two single layers of the coating. At longer distances, the heating of the surface by the flame is less, and massive oxidation does not take place.

The roughness at spray distances of 300 mm and above is always lower than $15 \mu\text{m}$ (Fig. 2b). Below 300 mm, the surface roughness increases up to $36 \mu\text{m}$ at 150 mm spray distance. This can be explained by the slow particles due to the short acceleration time.

The counted number of unmolten particles in the coatings is plotted in Fig. 4. This number increases slightly with longer spray distance, except for an outlier at 500 mm. At 400 mm, an average number of 85 unmolten particles is observed. At longer spray distances, the counted number of these particles reaches a value of up to 109 at 600 mm. This can be explained by the decreasing flame temperature with increasing distance from the nozzle exit, so that some particles solidify again before

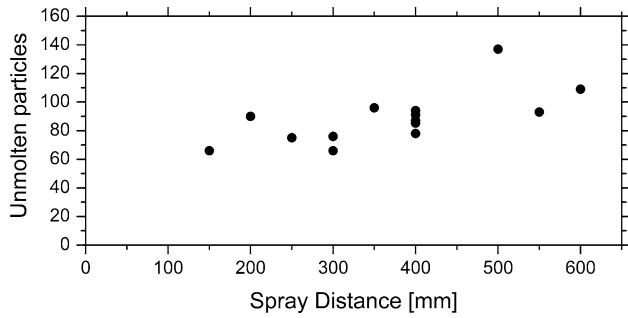


Fig. 4 Counted number of unmolten particles over a length of 10 mm, plotted over the spray distance. Fuel flow: 16.2 L/h, oxygen flow: 650 slpm

they hit the substrate. Consequentially, one would expect an increase in the amount of unmolten particles towards the lowest spray distance due to the low particle temperature (see above), but this could not be observed: Only 66 unmolten particles were counted in the coating over the whole measurement length of 10 mm at a spray distance of 150 mm. It is possible that the particles which spread away at short spray distances are mainly unmolten particles. They cannot be built into the coating and, hence, result in a lower amount of unmolten particles in the coating.

Summing up, a spray distance of 250 to 450 mm leads to particularly attractive coating properties with respect to the parameters porosity, roughness, and amount of unmolten particles.

3.3 Variation of Fuel and Oxygen Flow Rates

The fuel and oxygen flow rates control the flame temperature as well as the combustion chamber pressure p and thus the velocity of the exhaust gas. While higher fuel and oxygen flow rates lead to a higher chamber pressure, the ratio of fuel/oxygen flow affects the burning process and, hence, has an influence on the flame temperature as well as the pressure of the exhaust gas. The fuel/oxygen ratio is described by the equivalence ratio ϕ , defined as the quotient between the actual fuel/oxygen ratio of the process and the fuel/oxygen ratio under stoichiometric conditions (Ref 13). At an equivalence ratio <1 , the fuel is totally burnt, but the oxygen abundance might cause a higher oxidation of the coating, while at an equivalence ratio of >1 , the combustion is incomplete. At an equivalence ratio of 1, the flame and the particles reach their maximum temperature (Ref 13). In contrast, the combustion chamber pressure mainly affects the flame speed (Ref 8). A higher flame speed causes higher particle velocities, leading to reduced porosity of the coating, as discussed above.

With the coating equipment used in this study, the combustion chamber pressure cannot be adjusted directly. Only fuel and oxygen flows are adjustable. The pressure is measured in the coating equipment. Values for the equivalence ratio of 0.6 to 1.1 can be realized: At higher equivalence ratios, the combustion chamber pressure decreases too much since the fuel flow cannot be adjusted

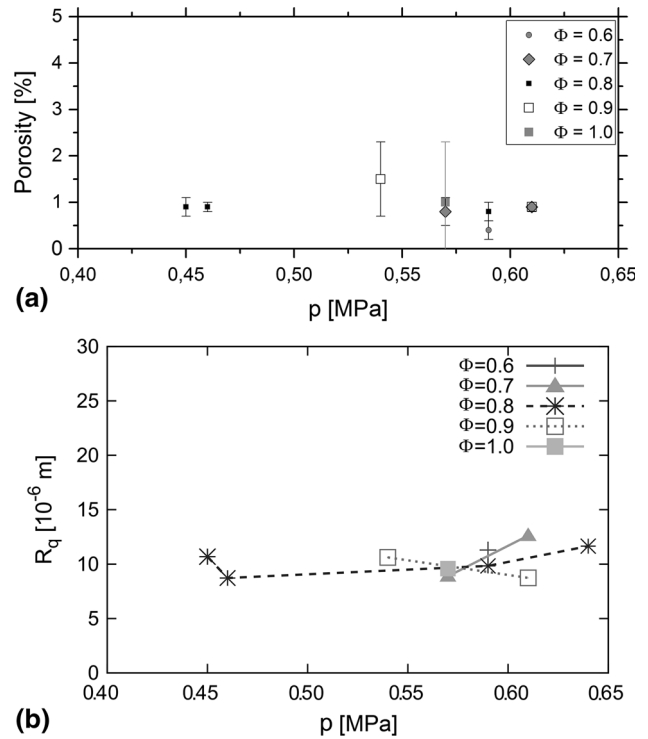


Fig. 5 Coating roughness and porosity at different combustion chamber pressures p and equivalence ratios ϕ . (a) Porosity. (b) Roughness

over a maximum value of 20 L/h and so the oxygen flow has to be reduced. The experiments in this section were carried out at a constant spray distance of 400 mm.

The measured values of the porosity at different equivalent ratios and different chamber pressures are summarized in Fig. 5(a). All coatings have a porosity of 1% or lower, except for the coating at a chamber pressure of 0.54 MPa and an equivalence ratio of 0.9, where the porosity is slightly higher (1.5%).

Figure 5(b) shows the surface roughness R_q of the coatings at different combustion chamber pressures p and equivalence ratios ϕ . The surface roughness is in the range between 9 and 13 μm for all values of p and ϕ . Apparently, combustion chamber pressure and equivalence ratio have little effect on porosity and roughness within the parameter range studied here.

Figure 6 shows a decrease of the amount of unmolten particles with increasing equivalence ratio. The reason is the lower flame temperature at lower equivalence ratio. At a stoichiometric combustion of $\phi=1.0$, the highest flame temperatures are reached (see above) and therefore even big particles or particles in the outer flame area can be melted.

The present work shows that the combustion chamber pressure has no significant effect on the coating structure. The equivalence ratio influences the melting of the particles and the amount of unmolten particles in the coating, but the maximum possible equivalence ratio is not necessary to form coatings with the required low porosity and

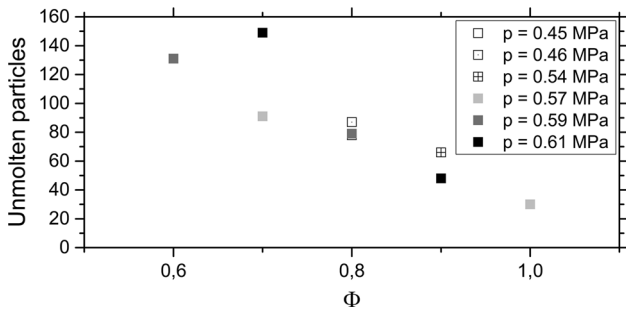
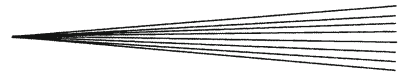


Fig. 6 Counted number of unmolten particles over a length of 10 mm, at different combustion chamber pressures p and equivalence ratios ϕ

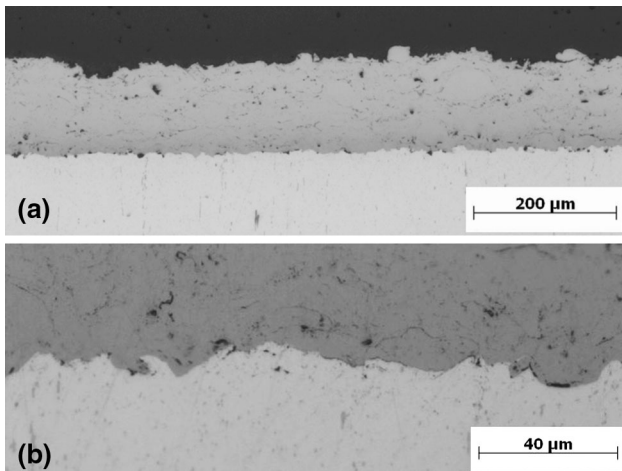


Fig. 7 Optical micrograph of the cross section of a NiCuCrAl coating (top) on a copper substrate, $\phi=0.8$, spray distance 400 mm, $p=0.45$ MPa. (a) whole coating. (b) Substrate/coating interface

intermediate roughness. Although the counted number of unmolten particles at lower equivalence ratios is higher than at $\Phi=1.0$, the unmolten particles are evenly distributed in the coating structure and the counted number is still low at an equivalence ratio of $\phi=0.8$. Hence, a lower equivalence ratio than $\phi=1.0$ can be chosen for further studies to avoid damage of the copper substrate by too high flame temperatures. Compared to the spray distance, the combustion chamber pressure and the equivalence ratio have a negligible effect on the porosity of the NiCuCrAl coating. In conclusion, a coating structure with required properties with the used coating equipment can be achieved for example with a fuel flow of 16.2 L/h, an oxygen flow of 650 slpm ($\phi=0.8$, $p=0.45$ MPa) and a spray distance of 400 mm. This parameter set is used for further studies.

3.4 Coating on Copper Substrates

In the above section, only the coating structure itself is considered. For further coating development, the adhesion of the NiCuCrAl coating on copper substrates has to

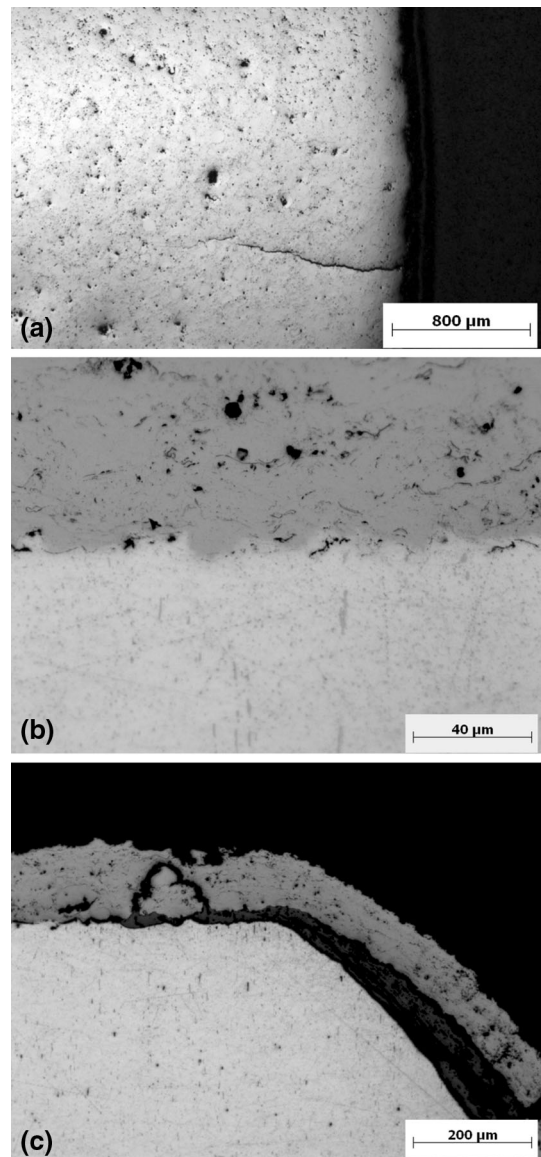


Fig. 8 Optical micrographs of the NiCuCrAl coating on Cu substrate after 20 laser cycles at 1100 °C for 10 s each and subsequent quenching in icy water. (a) Cross section parallel to the coating surface. (b) Interface substrate/coating. (c) Delamination at the edge of the specimen

be investigated. Based on the experiments above, a spray distance of 400 mm, fuel flow of 16.2 L/h, and an oxygen flow of 650 slpm ($\phi=0.8$, $p=0.45$ MPa) were chosen as optimized parameter set for further experiments. Figure 7 shows the cross section of a coated copper substrate. The interface porosity is sufficiently low, and only few oxide stringers can be observed in this micrograph. The coating material fills out most of the valleys of the substrate's surface roughness. The porosity of the coating is 0.8% and is similar to the measured porosity on steel substrates (1.0%, see Fig. 2a). Comparing Fig. 7(a) and 3(c), the coating structure on copper substrates is similar to the structure on steel substrates.

To investigate the adhesion of the coating to the substrate, laser flash experiments were carried out. These experiments were used in the past to characterize the adhesion of atmospheric plasma-sprayed NiCrAlY coatings on copper substrates. The coatings failed by delamination after only one cycle at a holding time of 500 °C for 2 s. In contrast, the NiCuCrAl coatings of this study showed no delamination after 15 cycles even at 1000 °C/2 s as holding conditions. In both cases, the specimens were air cooled.

To exacerbate the testing conditions, the duration of each cycle was increased to 10 s, and the samples were quenched in icy water subsequently. At 500 °C surface temperature, no failure or change in the coating structure was observed after 20 cycles. At 1100 °C, vertical cracks in the coating formed after 20 cycles (Fig. 8a), but the adhesion was still good (Fig. 8b). Only at the edges of the specimens, coating delamination due to edge effects was observed (Fig. 8c). It is assumed that the vertical cracks form due to stress relaxation at high temperatures and subsequent formation of tensile stresses at the coating upon rapid cooling. Further research has to be carried out to quantify this crack formation.

4. Conclusions

In this work, a new coating material Ni-30%Cu-6%Al-5%Cr is investigated for HVOF spraying. A variation of coating parameters was carried out to observe their influence on the coating structure. The main results are as follows:

- The coating surface roughness increases with decreasing spray distance.
- The porosity increases with low spray distances as well as at spray distances >500 mm.
- A spray distance of 250 to 450 mm was found to be ideal to form a dense coating with adequate surface roughness and amount of unmolten particles.
- The coating roughness and porosity are mainly influenced by the spray distance, while the amount of unmolten particles is mainly controlled by the equivalence ratio.
- An equivalence ratio of 0.8 can be used for further coating application to avoid substrate damage by high flame temperatures.

- Optimized coating process parameters were used to deposit the NiCuCrAl coating on a copper substrate, and excellent adhesion was demonstrated by a laser flash experiment.

Acknowledgements

The financial support has been provided by the German Research Foundation (Deutsche Forschungsgemeinschaft—DFG) in the framework of the Sonderforschungsbereich Transregio 40, Teilprojekt D2.

References

1. J.R. Riccius, O. Haidn, and E.B. Zametaev, Influence of Time Dependent Effects on the Estimated Life Time of Liquid Rocket Chamber Walls, AIAA, 2004
2. L.U. Ogbuji, Oxidation Behavior of Cu-Cr Environmental Barrier Coatings on Cu-8Cr-4Nb, *Surf. Coat. Technol.*, 2005, **197**(2-3), p 327-335
3. S.V. Raj, L.J. Ghosn, C. Robinson, and D. Humphrey, High Heat Flux Exposures of Coated GRCop-84 Substrates, *Mater. Sci. Eng. A*, 2007, **457**, p 300-312
4. J. Schloesser, M. Bäker, and J. Rösler, Laser Cycling and Thermal Cycling Exposure of Thermal Barrier Coatings on Copper Substrates, *Surf. Coat. Technol.*, 2011, **206**, p 1605-1608
5. T. Fiedler, T. Fedorova, J. Rösler, and M. Bäker, Design of a Nickel-Based Bond-Coat Alloy for Thermal Barrier Coatings on Copper Substrates, *Metals*, 2014, **4**, p 503-518
6. B. Rajasekaran, G. Mauer, and R. Vaßen, Enhanced Characteristics of HVOF-Sprayed MCrAlY Bond Coats for TBC Applications, *J. Therm. Spray Technol.*, 2011, **20**, p 1209-1216
7. E. Lugscheider, C. Herbst, and L. Zhau, Parameter Studies on High-Velocity Oxy-fuel Spraying of MCrAlY Coatings, *Surf. Coat. Technol.*, 1998, **108-109**, p 16-23
8. K. Isoyama, J. Kawakita, S. Kuroda, and H. Yumoto, Key Factors for Dense Copper Coating by HVOF Spraying, *Thermal Spray, ASM International*, 2003, **2003**, p 755-762
9. S. Bose, *High Temperature Coatings*, Elsevier, Amsterdam, 2007
10. S. Deshpande, S. Sampath, and H. Zhang, Mechanisms of Oxidation and its Role in Microstructural Evolution of Metallic Thermal Spray Coatings—Case Study for Ni-Al, *Surf. Coat. Technol.*, 2006, **200**, p 5395-5406
11. ImageJ, <http://rsb.info.nih.gov/ij/index.html>, 2015-06-09
12. C.-J. Li and W.-Y. Li, Effect of Sprayed Powder Particle Size on the Oxidation Behavior of MCrAlY Materials During High Velocity Oxygen-Fuel Deposition, *Surf. Coat. Technol.*, 2003, **162**, p 31-41
13. L. Pawlowski, *Science and Engineering of Thermal Spray Coatings*, Wiley, Hoboken, 2008